ORIGINAL ARTICLE

Medical Journal of Western Black Sea
Batı Karadeniz Tıp Dergisi

Med J West Black Sea 2026;10(2):277-288
DOI: 10.29058/mjwbs.1911696

Protective effects of 1,8-cineole against potassium dichromate-induced nephrotoxicity in rats: Evaluation of oxidative stress, inflammatory, and apoptotic pathways

Ratlarda potasyum dikromat kaynaklı nefrotoksisiteye karşı 1,8-sineolün koruyucu etkileri: Oksidatif stres, inflamatuvar ve apoptotik yolakların değerlendirilmesi

Tansu Kuşat[1], Feyza Başak[1], Eyüp Altınöz[2], Yasemin Biçer[2]

[1]Karabük University, Faculty of Medicine, Department of Histology and Embryology, Karabük, Türkiye
[2]Karabük University, Faculty of Medicine, Department of Medical Biochemistry, Karabük, Türkiye

Cite this article as: *Kuşat T et al. Protective effects of 1,8-cineole against potassium dichromate-induced nephrotoxicity in rats: Evaluation of oxidative stress, inflammatory, and apoptotic pathways. Med J West Black Sea. 2026;10(2):277-288.*

ABSTRACT

Aim: Potassium dichromate is a heavy metal associated with nephrotoxicity in people and animals, resulting in oxidative stress, inflammation, and apoptosis in tissues. 1,8-cineole is a monoterpene with antioxidant, anti-inflammatory, and anti-apoptotic properties. This study aimed to investigate the potential protective effects of 1,8-cineole against potassium dichromate-induced nephrotoxicity.

Material and Methods: This study involved 40 male Wistar albino rats, randomly allocated to five groups (n=8): control, vehicle, potassium dichromate (PD), 1,8-cineole (CN), and potassium dichromate combined with 1,8-cineole (PD+CN). All treatments were administered orally once daily for 28 days. Malondialdehyde (MDA), reduced glutathione (GSH), catalase (CAT), and superoxide dismutase (SOD) levels were assessed as oxidative stress in kidney tissue. Furthermore, levels of nuclear factor kappa B (NF-κB) and tumor necrosis factor-alpha (TNF-α) were evaluated as indicators of inflammation. Bax expression was analyzed through immunohistochemical methods, and histopathological changes in kidney tissue were assessed.

Results: In the kidney tissue of rats in the PD group, elevated levels of MDA, NF-κB, and TNF-α were noted relative to other experimental groups, although activities of GSH, SOD, and CAT were decreased ($p<0.01$). CN treatment led to substantial enhancements in GSH, SOD, and CAT levels, concurrently reducing MDA, NF-κB, and TNF-α levels ($p<0.01$). Immunohistochemical investigations showed that PD increased Bax expression in kidney tissue ($p<0.01$), but CN treatment significantly reduced Bax expression ($p<0.01$). In the PD+CN group, kidney tissue histopathological changes caused by PD were reduced.

Conclusion: CN has anti-inflammatory, antioxidant, anti-apoptotic, and nephroprotective properties against PD-induced nephrotoxicity.

Keywords: 1,8-cineole, inflammation, nephrotoxicity, oxidative stress, potassium dichromate

ÖZ

Amaç: Potasyum dikromat, insanlar ve hayvanlarda nefrotoksisite ile ilişkilendirilen, dokularda oksidatif stres, inflamasyon ve apoptoza yol açan ağır bir metaldir. 1,8 sineol ise anti-oksidan, anti-inflamatuar ve anti-apoptotik aktivitelere sahip bir monoterpendir. Bu çalışmada, potasyum dikromat kaynaklı böbrek toksisitesine karşı 1,8 sineol'ün olası koruyucu etkilerinin incelenmesi amaçlanmıştır.

Gereç ve Yöntemler: Bu çalışmada 40 adet Wistar albino ırkı erkek sıçan rastgele olarak kontrol, vehicle, potasyum dikromat (PD), 1,8-sineol (CN) ve potasyum dikromat + 1,8-sineol (PD+CN) olmak üzere beş gruba ayrıldı (n=8). Tüm uygulamalar 28 gün boyunca günde bir kez oral yolla gerçekleştirildi. Böbrek dokusunda oksidatif stresin biyokimyasal belirteçleri olarak malondialdehit (MDA), indirgenmiş glutatyon (GSH), katalaz (CAT) ve süperoksit dismutaz (SOD) düzeyleri değerlendirildi. Ayrıca inflamatuvar parametreler olarak nükleer faktör kappa B (NF-κB) ve tümör nekroz faktör-alfa (TNF-α) düzeyleri analiz edildi. Apoptotik sürecin değerlendirilmesi amacıyla Bax ekspresyonu immünohistokimyasal yöntemle incelendi ve böbrek dokusunda oluşan histopatolojik değişiklikler değerlendirildi.

Bulgular: PD grubu sıçanların böbrek dokusunda diğer deney gruplarına göre MDA, NF-κB ve TNF-α seviyelerinde artış gözlemlenirken, GSH, SOD ve CAT aktivitelerinde azalma görüldü ($p<0.01$). CN tedavisi, MDA, GSH, SOD ve CAT seviyelerinde önemli iyileşmeler sağlarken, NF-κB ve TNF-α seviyelerini düşürdü ($p<0.01$). İmmünohistokimyasal incelemeler, PD'nin böbrek dokusunda apoptotik belirteçlerden biri olan Bax ekspresyonunu artırdığını ($p<0.01$), CN tedavisinin ise Bax ekspresyonunu önemli ölçüde azalttığını gösterdi ($p<0.01$). Buna ek olarak, PD'nin böbrek dokusunda neden olduğu belirgin histopatolojik değişiklikler, PD+CN grubunda hafifledi.

Sonuç: Çalışmamızın sonuçları, CN'nin PD kaynaklı nefrotoksisite üzerinde antiinflamatuar, antioksidatif, antiapoptotik ve nefroprotektif etkileri olduğunu göstermektedir.

Anahtar Kelimeler: 1,8-sineol, İnflamasyon, nefrotoksisite, oksidatif stres, potasyum dikromat

Corresponding Author: Tansu Kusat ✉ tansukusat@karabuk.edu.tr
Received: 17.03.2026 **Revision:** 05.06.2026 **Accepted:** 03.08.2026

Copyright © 2026 The Author(s). Published by Zonguldak Bülent Ecevit University. This is an open access article distributed under the Creative Commons Attribution License (CC BY), which permits unrestricted use, distribution, and reproduction in any medium or format, provided the original work is properly cited.

Highlights

- Potassium dichromate induced nephrotoxicity in rat kidney tissue.
- 1,8-Cineole significantly reduced oxidative stress markers in renal tissue.
- 1,8-Cineole suppressed nuclear factor kappa B (NF-κB) and tumor necrosis factor-alpha (TNF-α) mediated inflammatory responses.
- Bax expression and apoptotic activity were reduced by 1,8-cineole treatment.
- 1,8-Cineole improved histopathological alterations in PD-induced renal damage.

INTRODUCTION

Chromium (Cr) is a heavy metal that presents considerable hazards to human health owing to its poisonous characteristics (1). Cr toxicity is contingent upon its chemical form, dosage, and duration of exposure (2). Cr is typically present in the environment in its trivalent [Cr(III)] and hexavalent [Cr(VI)] forms (3). Cr(VI) is known to traverse cell membranes readily through anion transporter systems and is subsequently reduced to Cr(III) within the cell by the generation of reactive intermediates (4). It has been reported that the intermediates produced during this reduction process serve as electron donors in Fenton and Haber–Weiss reactions, resulting in the production of an inordinate quantity of reactive oxygen species (ROS). Increased ROS formation is reported to trigger oxidative stress mechanisms, causing damage to cellular macromolecules and contributing to the development of toxicity in many vital organs (5,6).

Potassium dichromate (PD) is a Cr(VI) compound extensively utilized in numerous industrial applications, such as leather tanning, electroplating, industrial pigments, and the stainless steel sector (7). Numerous investigations have associated this compound with multi-organ toxicity, teratogenicity, mutagenicity, and carcinogenicity (1,8). Moreover, due to the kidneys' essential function in the excretion of PD and the compound's propensity to accumulate in renal tissue, the kidneys have emerged as the principal organ of focus in research examining PD-induced damage (2,9). Experimental investigations indicate that PD exposure induces kidney damage and nephrotoxicity by excessive generation of ROS, activation of inflammatory responses, and stimulation of apoptotic pathways (10-12).

Excessive ROS production from PD undermines cellular antioxidant defense mechanisms, resulting in oxidative stress and initiating lipid peroxidation, protein oxidation, and DNA damage (6,13). It has also been reported that PD-induced ROS production and the resulting oxidative stress trigger the activation of inflammatory signaling pathways such as nuclear factor kappa B (NF-κB (12)); this, in turn, can contribute to the exacerbation of the inflammatory response by causing an increase in the expression of various pro-inflammatory cytokines, primarily tumor necrosis factor-α (TNF-α) (2,14). Moreover, NF-κB-mediated inflammatory activation is documented to correlate with elevated expression of pro-apoptotic proteins (Bax) and to initiate the apoptotic process (15,16). Therefore, the interaction between oxidative stress, NF-κB-mediated inflammation, and apoptosis plays a critical role in understanding the molecular mechanisms of PD-related nephrotoxicity.

Kidney diseases are among the foremost global health issues; thus, research into the production of natural nephroprotective medicines is becoming increasingly significant (1,17). Eucalyptol, or 1,8-cineol (CN), is a saturated monoterpene derived from the essential oils of several plants, including eucalyptus, bay leaf, camphor, wormwood, sweet basil, rosemary, tea tree, and tansy (18-20). This monoterpene is recognized for a high safety profile (21) and has been approved for human use by the United States Food and Drug Administration (FDA) in areas including cosmetics, aromatherapy, dentistry, and flavoring (19). A number of investigations have demonstrated that the pharmacological benefits of CN principally arise from its capacity to suppress oxidative stress, inflammation, and apoptosis (18,20,22,23). Moreover, it is asserted that CN's antioxidant and anti-inflammatory properties are mediated by the modulation of NF-κB signaling pathways (18,22).

Although studies evaluating the effects of 1,8-cineol on nephrotoxicity caused by various agents exist today, no studies investigating its potential effects against PD-induced kidney toxicity, which is the focus of our research, have been found. In this context, the present study aimed to evaluate the nephroprotective potential of 1,8-cineol in PD-induced nephrotoxicity through biochemical, histopathological, and immunohistochemical analyses.

MATERIAL and METHODS

Chemicals

Potassium dichromate (K2Cr2O7, ≥99.5% purity, P5271) was acquired from Sigma-Aldrich (Darmstadt, Germany), and 1,8-cineole (>98% purity, 470-82-6) was obtained from Tokyo Chemical Industry Co. Ltd., Japan.

Ethical Approval and Animal Supply

In this investigation, 40 male Wistar Albino rats, each weighing approximately 200-220 g, were acquired from the Experimental Medicine and Application unit of Karabük University. All research protocols, including the utilization of animals, received approval from the Karabük University Experimental Animal Use and Ethics Committee (Protocol No: 2025/10/33). The animals were provided ad libitum access to normal rat chow under artificial lighting (12-hour dark/light cycle), adequate ventilation, a mean temperature of 21 ± 1 °C, and relative humidity of 50-60%, while housed in clean standard cages with unrestricted access to water.

Experimental Design

The animals were randomly allocated into five groups (n=8), and all rats participating in the study were weighed on the initial day of the trial using a precision balance, with their live weights documented.

1) Control Group: Rats in this group received isotonic saline solution via gavage for a duration of 28 days, commencing on the initial day of the study.

2) Vehicle Group: Rats in this group received 1 ml of physiological saline containing 2% Tween 80 via gavage for a duration of 28 days, commencing on the initial day of the study.

3) Potassium Dichromate (PD) Group: Rats in this group received potassium dichromate (15 mg/kg) dissolved in isotonic saline solution via gavage daily for 28 days (24).

4) 1,8 Cineol (CN) Group: Rats in this group received 1,8 Cineol (200 mg/kg) in 1 ml of physiological saline with 2% Tween 80 via gavage daily for 28 days (23).

5) PD+CN Group: Rats in this group received potassium dichromate (15 mg/kg) dissolved in isotonic saline solution via gavage once daily for 28 days, followed one hour later by 1 ml of physiological saline containing 2% Tween 80 and 1,8-cineole (200 mg/kg).

Collecting Tissue Samples

Upon completion of the final procedures, the rats in all groups were weighed, and their life weights were documented. Rats were euthanized via cervical dislocation while under anesthesia with ketamine (80 mg/kg) and xylazine (8 mg/kg). Kidney tissue specimens were extracted from the euthanized animals. Certain kidney tissue samples were rinsed with saline to assess biochemical parameters and subsequently stored at -80 °C till measurement of the biochemical parameters was conducted. The residual kidney tissue samples were immersed in a 10% formalin solution and fixed for 48 hours. Upon concluding the fixation process, the tissues were subjected to a 24-hour wash with running tap water, subsequently dehydrated in ascending concentrations of alcohol (70%, 80%, 96%, 100%), cleaned with xylene, and embedded in paraffin. Serial slices measuring 5-6 µm were obtained from paraffin blocks utilizing a microtome and subsequently placed onto Poly L-lysine-coated slides for light microscopy and immunohistochemical analyses.

Biochemical Analysis

Kidney tissue samples were homogenized in phosphate buffer at 12,000 rpm on ice for 1-2 minutes using an IKA Ultra Turrax T 25 basic (IKA Labortechnik, Staufen, Germany). MDA levels were quantified in the homogenate, and the residual homogenate was subjected to centrifugation at 3000 rpm at +4 °C for 20 minutes to isolate the supernatant. All additional biochemical studies were conducted on the acquired supernatant. The MDA analysis was conducted following the methodology outlined by Altınoz et al. (25). The fundamental premise of the approach involves measuring the absorbance of the pink hue produced from the interaction between MDA and thiobarbituric acid (TBA) at 535 nm. N-butanol served as a blank, whereas tetramethoxypropane functioned as a standard. Results were quantified as nanomoles per gram of wet tissue.

The GSH level was assessed using the method outlined by Keelo et al. (26). The fundamental premise of the approach involves quantifying the absorbance of the green-yellow hue produced from the interaction between GSH and 5,5′-dithiobis(2-nitrobenzoic acid) (DTNB) at 412 nm. Distilled water served as a blank, and the results were reported as nanomoles per gram of wet tissue.

The measurement of SOD activity was conducted utilizing the methodology described by Ozturk et al. (27). The fundamental principle of the method relies on the generation of superoxide radicals through the xanthine-xanthine oxidase reaction, followed by the formation of a purple-blue product via the reduction of nitroblue tetrazolium (NBT) by the superoxide radicals. The absorbance of the resultant formazan at 560 nm is utilized to quantify SOD activity. The SOD activity was quantified in U/g of protein.

The measurement of CAT activity was conducted using the methodology described by Ozturk et al. (27). The fundamental principle of the method is that the decomposition of H_2O_2 in the H_2O_2-phosphate buffer, facilitated by the CAT enzyme in the supernatant, results in a reduction in absorbance at 240 nm. The recorded decrease in absorbance was monitored over a duration of 1 minute to assess enzyme activity. CAT activity was quantified as K per gram of protein.

In addition, NF-κB (Catalog No: E0287Ra) and TNF-α (Catalog No: E0764Ra) concentrations were assessed using an ELISA kit.

Histopathological Analysis

Kidney tissues were preserved in 10% formaldehyde for 48 hours. The samples were subsequently rinsed overnight

with running tap water, dehydrated using a 50-100% ethanol series, and subjected to a xylene series. The specimens were subsequently embedded in paraffin. Serial slices of 5 µm thickness were obtained from the paraffin blocks, and Masson trichrome staining was used to assess the general histological architecture. Picrosirius Red staining was conducted to evaluate collagen deposition and interstitial fibrotic alterations in the renal tissue. All sections were analyzed using a light microscope. The parameters evaluated for the severity of kidney damage were tubular degeneration and dilatation across 10 different areas per section, interstitial inflammatory cell infiltration, and alterations in the glomeruli. Kidney tissue damage was classified as none (0), mild (1), moderate (2), and severe (3). The maximal histopathological damage score (MHDS) was 12. All sections were analyzed utilizing a Leica 2500 DM LED light microscope and LAS Analysis system (Leica, Germany).

Immunohistochemical Analysis

Immunohistochemical staining was conducted utilizing the streptavidin-biotin-peroxidase complex (sABC) technique with Bax antibody. Following deparaffinization of the sections via a xylene series, they were subjected to a decreasing alcohol series (100-70%) and subsequently transferred to distilled water. For antigen retrieval, the sections immersed in citrate buffer (Bio-Optica, 15-M103, pH 6) were subjected to boiling in a microwave oven (600 W) for 15 minutes, after which hydrogen peroxide (0.3% H2O2) was applied to the sections and allowed to incubate for 20 minutes. Subsequent to the addition of protein blocks and a 5-minute incubation, the sections were treated with anti-Bax primary antibody (Santa Cruz, 1/100 dilution) and incubated for 2 hours at +4˚C in a humid atmosphere. Subsequent to this stage, slices were incubated with a secondary antibody for 30 minutes, followed by a 30-minute incubation with a streptavidin horseradish peroxidase complex, and then treated with a substrate-chromogen (DAB; diaminobenzidine) solution until a brown response was evident. Mayer's hematoxylin stain was utilized on the sections as a nuclear stain, followed by a passage through an alcohol-xylene series and sealed with Entellan. All intermediate washes were conducted using phosphate-buffered saline (PBS). In accordance with the kit protocol, cells exhibiting immunoreactivity to anti-Bax were subjected to semi-quantitative analysis using a Leica 2500 DM light microscope. In order to assess immunohistochemical staining, semi-quantitative H-scores were assessed by counting positively stained cells in five arbitrarily selected areas for each group (H-score: ∑Pi (i + 1)) (Pi: the percentage of cells that are positively stained; i: the intensity of the staining) (27).

Statistical Analysis

Statistical data analysis was conducted utilizing IBM SPSS Statistics version 25.0 for Windows. The Kolmogorov-Smirnov test was employed to ascertain if the data exhibited a normal distribution (p>0.05). If the data exhibited a normal distribution, statistical analysis was conducted utilizing One-Way ANOVA, followed by the Tukey post hoc test for multiple comparisons. Results were expressed as mean ± standard deviation (Mean±SD), with a P<0.01 value deemed statistically significant.

RESULTS

Results of Average Body Weights

On the initial day of the experiment, no statistically significant difference in average live weights was observed across the groups (Figure 1, p>0.05). On the 28th day, the measurement of live body weight indicated a statistically significant reduction in average live body weight in the PD group relative to the other experimental groups (Figure 1, p<0.01). The PD+CN group exhibited a statistically significant increase in average live body weight compared to the PD group (Figure 1, p<0.01). No statistically significant difference in average live weights was observed among the control, vehicle, and CN groups (Figure 1, p>0.05).

Results of Biochemical Analysis

Results of oxidative stress markers in kidney tissue

Levels of MDA, GSH, CAT, and SOD, regarded as biochemical markers of oxidative stress in kidney tissue, were assessed. The evaluations indicated that GSH levels and the activities of CAT and SOD were statistically considerably

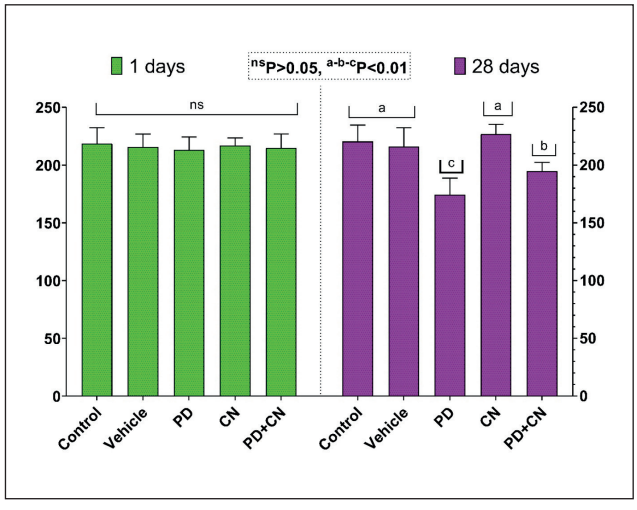

Figure 1: Average live body weights on days 1 and 28 of the experiment. Data are expressed as the arithmetic mean ± SD (n = 8). [a-b-c] The superscripts explain the statistically significant difference (p<0.01). [c]PD compared with [a]Control, [a]Vehicle, [a]CN, and [b]PD+CN (p<0.01), [b]PD+CN compared with [a]Control, [a]Vehicle, and [a]CN (p<0.01). [ns] Indicates no statistically significant difference between groups (p>0.05).

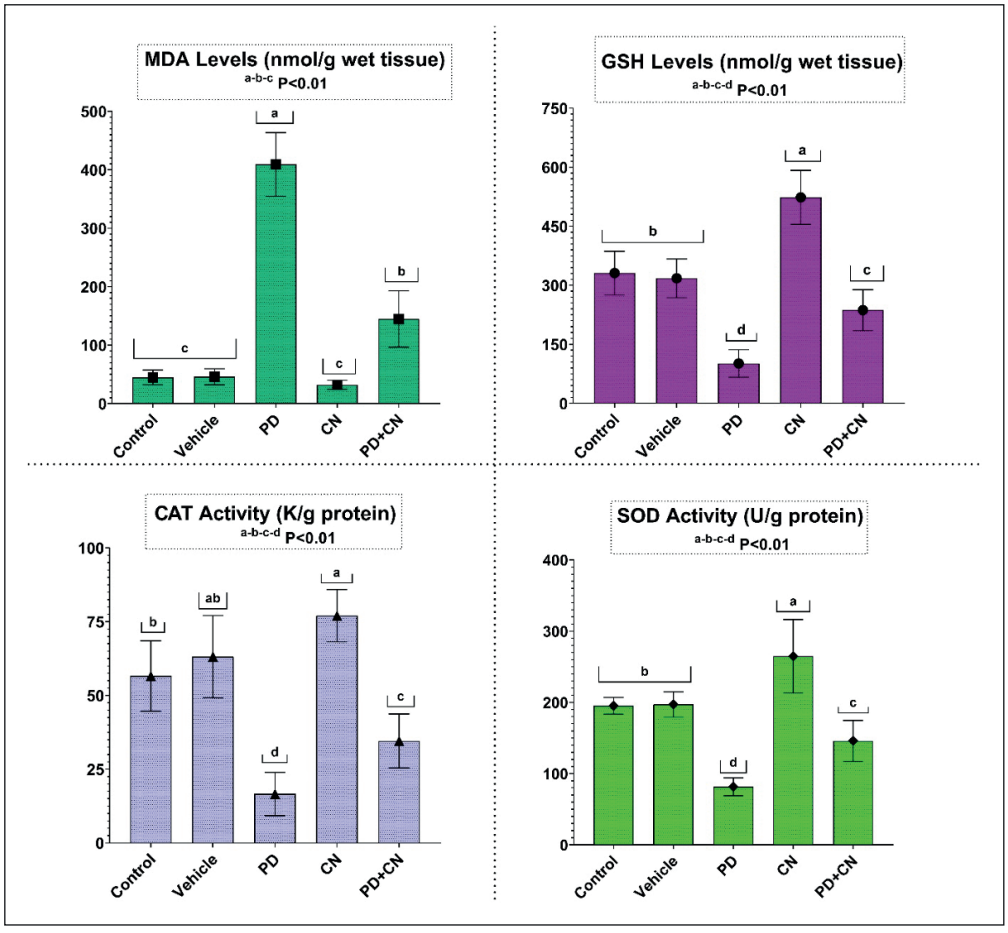

Figure 2: Results of MDA and GSH levels and CAT and SOD activities in kidney tissue. Data are expressed as the arithmetic mean ± SD (n = 8). [a-b-c] The superscripts explain the statistically significant difference (p<0.01): **MDA**; [a]PD compared with [c]Control, [c]Vehicle, [c]CN, and [b]PD+CN (p<0.01), [b]PD+CN compared with [c]Control, [c]Vehicle, and [c]CN (p<0.01). **GSH and SOD;** [d]PD compared with [b]Control, [b]Vehicle, [a]CN, and [c]PD+CN (p<0.01), [c]PD+CN compared with [b]Control, [b]Vehicle, and [a]CN (p<0.01), [a]CN compared with [b]Control, and [b]Vehicle (p<0.01). **CAT;** [d]PD compared with [b]Control, [ab]Vehicle, [a]CN, and [c]PD+CN (p<0.01), [c]PD+CN compared with [b]Control, [ab]Vehicle, and [a]CN (p<0.01), [a]CN compared with [b]Control (p<0.01).

reduced in the PD group relative to the other experimental groups, whereas MDA levels were markedly elevated in the PD group compared to the others (Figure 2, p<0.01). In the PD+CN group, levels of GSH and activity of CAT and SOD were elevated relative to the PD group, whereas MDA levels considerably decreased (Figure 2, p<0.01). The CN group exhibited the greatest levels of GSH and activities of SOD and CAT across all experimental groups, with statistically significant differences noted in comparison to the PD and PD+CN groups (Figure 2, p<0.01). No statistically significant differences were detected in MDA levels among the control, carrier, and CN groups; likewise, GSH levels and CAT and SOD activities showed no statistically significant differences between the control and vehicle groups (Figure 2, p>0.05).

Results of NF-κB and TNF-α levels in kidney tissue

The analysis of NF-κB and TNF-α levels in kidney tissue revealed a statistically significant elevation in the PD group relative to all other groups (Figure 3, p<0.01). The PD+CN group had markedly reduced levels of NF-κB and TNF-α in comparison to the PD group (Figure 3, p<0.01). No statistically significant difference was seen in NF-κB and TNF-α levels among the control, vehicle, and CN groups (Figure 3, p>0.05).

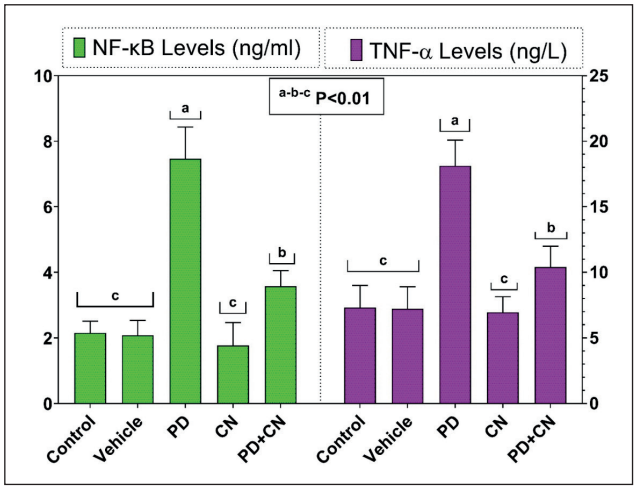

Figure 3: Results of NF-κB and TNF-α levels in kidney tissue. Data are expressed as the arithmetic mean ± SD (n = 8). [a-b-c] The superscripts explain the statistically significant difference ($p<0.01$). [a]PD compared with [c]Control, [c]Vehicle, [c]CN, and [b]PD+CN ($p<0.01$), [b]PD+CN compared with [c]Control, [c]Vehicle, and [c]CN ($p<0.01$).

Histopathological Findings

Masson's Trichrome and Picro Sirius Red staining results

Light microscopy of Masson's trichrome-stained sections demonstrated normal histological architecture in the glomeruli and tubular structures of the control, vehicle, and CN groups. The interstitial gaps in these groups appeared normal, and no major histological alterations were noted (Figure 4). The PD group exhibited notable histological alterations in comparison to the other groups. The alterations encompassed significant tubular dilatation, degradation of tubular epithelium, cytoplasmic vacuolization, extensive interstitial inflammatory cell infiltration, and glomerular degeneration (Figure 4). Moreover, there was a notable expansion of the interstitial spaces and a disruption of the regular tubular architecture. In the PD+CN group, renal morphology was comparatively maintained in contrast to the PD group. In this cohort, tubular degradation and dilation were less evident, interstitial inflammatory cell infiltration was less, and glomerular structures were maintained in comparison to the PD group (Figure 4).

Picrosirius red staining indicated normal collagen fiber density in the perivascular and periglomerular areas, with no interstitial fibrosis observed in the control, vehicle, and CN groups (Figure 4). Conversely, the PD group exhibited a dense accumulation of collagen fibers surrounding the dilated tubules and infiltrating the interstitial spaces relative to the control groups; this indicates that fibrotic alterations occur in kidney tissue due to PD exposure (Figure 4). In the treatment group where PD and CN were administered concurrently (PD+CN), collagen buildup was markedly diminished, suggesting that CN administration exerts a protective effect against PD-induced fibrotic alterations in the kidney (Figure 4).

Table 1 presents the histopathological damage scores in renal tissue across the groups. The damage score in the PD group was markedly elevated relative to the Control, Ve-

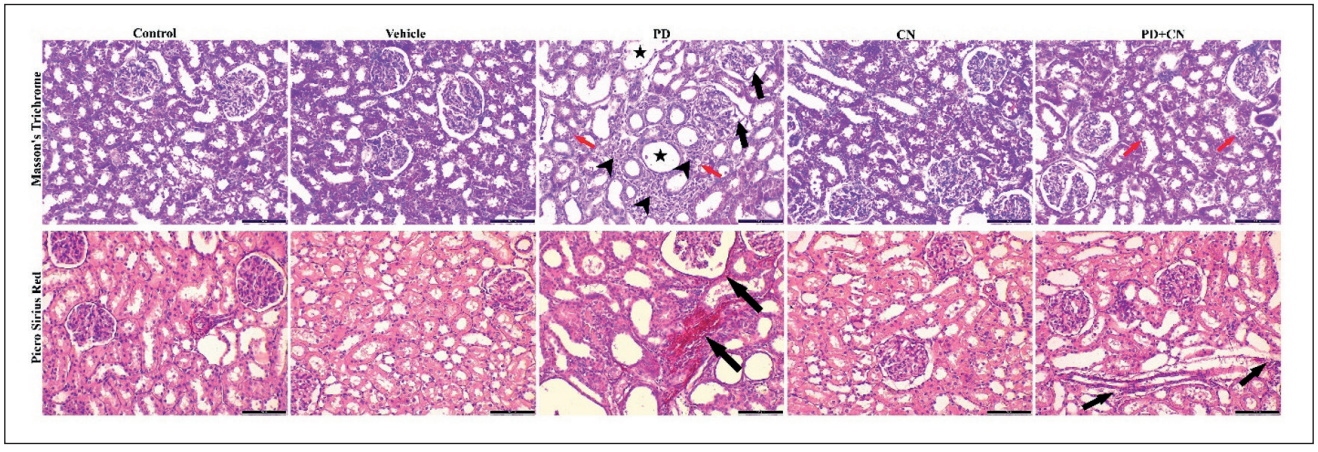

Figure 4: Images of Masson's Trichrome and Picro Sirius Red stained sections of the kidney tissue. The upper panels display Masson's trichrome staining (scale bar: 100 μm), revealing that the control, vehicle, and CN groups exhibit kidney architecture with typical glomerular and tubular structures. In the PD group, notable histological alterations were identified, comprising tubular dilatation (asterisk), tubular degeneration and cytoplasmic vacuolization (red arrows), degenerative modifications in the glomeruli (black arrow), and extensive interstitial inflammatory cell infiltration (arrowhead).In the PD+CN group, tubular architecture was comparatively maintained, and tubular degenerative alterations were less relative to the PD group. Picro Sirius Red staining is depicted in the lower panels, with a scale bar of 100 μm.In the PD group, collagen accumulation in interstitial spaces is indicated (black arrows), whereas collagen deposition is diminished in the PD+CN groups.

Table 1: The mean histopathological kidney damage score (MHDS) of all groups. Data are expressed as the arithmetic mean ± SD (n = 8).

Groups	Kidney Tissue MHDS
Control	1.19±0.41[c]
Vehicle	1.40±0.32[c]
PD	8.00±0.84[a]
CN	1.29±0.33[c]
PD+CN	4.21±0.46[b]

MHDS: mean histopathological damage score. [a-b-c] The superscripts explain the statistically significant difference ($p<0.01$). [a]PD compared with [c]Control, [c]Vehicle, [c]CN, and [b]PD+CN ($p<0.01$), [b]PD+CN compared with [c]Control, [c]Vehicle, and [c]CN ($p<0.01$).

Table 2: The H-Scores of Bax immunoreactivity. Data are expressed as the arithmetic mean ± SD (n = 8).

Groups	Bax H-Scores
Control	34.50±5.71[c]
Vehicle	38.13±6.47[c]
PD	166.63±11.72[a]
CN	37.38±5.80[c]
PD+CN	98.25±10.28[b]

[a-b-c] The superscripts explain the statistically significant difference: [a]PD compared with [c]Control, [c]Vehicle, [c]CN, and [b]PD+CN ($p<0.01$), [b]PD+CN compared with [c]Control, [c]Vehicle, and [c]CN ($p<0.01$).

hicle, and CN groups ($p<0.01$). The damage score in the PD+CN group was statistically substantially lower than that in the PD group ($p<0.01$).

Results of Immunohistochemistry Staining

Immunohistochemical investigations revealed that Bax immunoreactivity in the tubular epithelial cells of the Control, Vehicle, and CN groups displayed only mild cytoplasmic staining (Figure 5). No substantial difference was observed in H-scores among these groups (Table 2, $p>0.05$). The PD group had a considerable increase in Bax expression, indicated by pronounced cytoplasmic staining in renal tubular epithelial cells (Figure 5), with H-score values significantly elevated compared to the other groups (Table 2, $p<0.01$). In the PD+CN group, Bax immunoreactivity exhibited mild-to-moderate staining (Figure 5), with H-score values considerably lower than those in the PD group (Table 2, $p<0.01$).

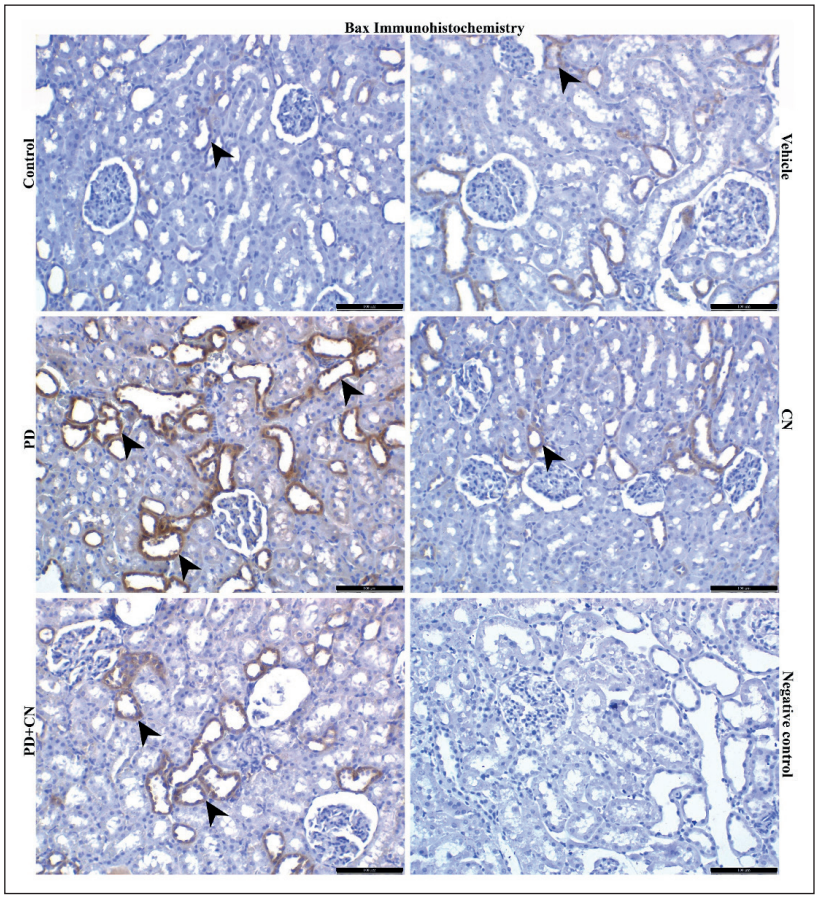

Figure 5: Images of Bax immunohistochemistry staining in kidney tissue. Arrowhead: Shows Bax immunoreactivity in renal tubules. Scale bar: 100 μm.

DISCUSSION

PD is a toxic Cr(VI) compound regarded as a major pollutant concerning environmental and occupational exposure, and is extensively utilized in numerous industrial processes (28). PD is known to readily infiltrate the human body via inhalation, ingestion, and dermal contact (29), leading to significant toxicities in both people and animals, including hepatotoxicity, nephrotoxicity, pulmonary toxicity, and cardiotoxicity (30-33).

Numerous studies on exposure to Cr(VI) compounds in humans and experimental animals have revealed that the kidney, as the primary Cr excretory organ, is an essential target organ (34), and that exposure to this chemical induces nephrotoxicity (10,35,36). Furthermore, numerous investigations have demonstrated that ROS generation, oxidative stress, apoptosis, and inflammation play important roles in the pathophysiology of PD-induced nephrotoxicity (1,17,37). In this respect, our current study examined the oxidative stress, inflammation, and apoptotic axis induced by PD exposure using biochemical, histological, and immunohistochemical methods.

Oxidative stress is linked to a variety of degenerative disorders, including kidney damage (17), and it has been determined that elevated oxidative stress inhibits the body's antioxidant defense system (especially SOD, GSH, and CAT) (26) and causes lipid peroxidation (high MDA levels) (17,38). A study investigating the nephroprotective properties of Echinacea purpurea against PD-induced nephrotoxicity in rats indicated that PD exposure diminished levels of GSH, SOD, and CAT, and significant histopathological alterations, including cortical tubular and epithelial degeneration as well as atrophic glomeruli, were noted in the kidney cortex (15). Another research investigation examining the potential protective effects of simvastatin against Cr(VI)-induced nephrotoxicity concluded that Cr(VI) exposure markedly elevated MDA levels, reduced GSH levels, and resulted in severe histopathological alterations, notably cortical tubular necrosis (39). In Sprague Dawley rats, the administration of PD through drinking water at several concentrations (0, 30, 100, and 300 mg/L) over a duration of 4 weeks was observed to elevate MDA levels in a dose-dependent manner and concurrently reduce live body weight in rats by the conclusion of the fourth week (40). A study determining the protective effect of ferulic acid against Cr(VI)-induced nephrotoxicity revealed that a 10-day exposure to 15 mg/kg body weight of Cr(VI) disrupted redox balance, elevated MDA levels, significantly reduced GSH and CAT activities, and resulted in tubular damage and glomerular dysfunction (41).

In our present investigation, we aimed to evaluate oxidative stress in rats by examining the nephrotoxicity of PD exposure through the measurement of MDA and GSH levels, as well as SOD and CAT activities. Our assessments indicated that the administration of 15 mg/kg PD to rats over 28 days elevated oxidative stress in renal tissue, leading to a notable increase in MDA levels (a byproduct of lipid peroxidation) relative to other groups, and a reduction in the average body weight of PD group rats by the conclusion of the experiment. Moreover, PD exposure in rats resulted in the failure of the antioxidant defense system in renal tissue, with substantial reductions in both enzymatic (SOD and CAT) and non-enzymatic (GSH) antioxidant levels. In accordance with prior research, our histological assessments revealed pronounced tubular dilatation, degradation of tubular epithelium, extensive interstitial inflammatory cell infiltration, and substantial fibrotic alterations in the renal tissue of the PD group rats.

Oxidative stress, along with inflammatory response and apoptosis, is among the key mechanisms involved in the development of PD-induced nephrotoxicity (4,41). TNF-α is recognized as a crucial cytokine in the initiation of the inflammatory response (2), while NF-κB is identified as the primary inflammatory transcription factor that governs the expression of this and other related pro-inflammatory cytokines (23,41,42). Moreover, NF-κB is regarded as an intracellular sensor of oxidative stress (43). Studies have shown that oxidative stress resulting from PD exposure triggers NF-κB activation, which in turn increases the expression of several pro-inflammatory cytokines, particularly TNF-α, contributing to the development of an inflammatory response (2,4,41,43). Moreover, it has been reported that the activation of NF-κB-mediated inflammatory signaling pathways can induce cellular apoptosis mechanisms and contribute to the progression of cellular damage by increasing the expression of pro-apoptotic proteins, such as Bax (43,44). Indeed, Karhib et al. reported that rats exposed to PD showed a significant increase in NF-κB levels in kidney tissue, along with increased levels of Bax and TNF-α (15). Therefore, in our current study, we decided to measure NF-κB, TNF-α, and Bax levels to determine the level of pro-apoptosis and inflammation in rats exposed to PD. The results of our investigation align with the aforementioned mechanism, revealing a substantial elevation in NF-κB and TNF-α levels in the kidney tissue of rats administered PD. Moreover, our immunohistochemistry consideration revealed an elevation in Bax expression within the renal tissue of rats in the PD group.

Given this information, it is crucial to formulate strategies for managing oxidative stress, inflammation, and apoptosis, as well as regulating biochemical and histopathological alterations in kidney tissue through the use of an effective therapeutic agent to combat PD-induced nephrotoxicity.

Medicinal plants provide a durable therapeutic strategy against chemical toxins. CN, referred to as eucalyptol or

1,8-epoxy-p-methane, is a monoterpene present in numerous plants (45). Studies have shown that this compound is considered safe (46) and its pharmacological effects stem particularly from its ability to suppress ROS production, oxidative stress, inflammation, and apoptosis (23,47-49). Moreover, it has been reported that CN influences its anti-inflammatory and antioxidant properties through the modulation of the NF-κB pathway (18).

Besides its antioxidant and anti-inflammatory properties, CN is additionally suggested to regulate apoptotic processes. Apoptosis is a crucial mechanism of programmed cell death that contributes to the maintenance of cellular homeostasis, with Bax identified as a primary regulator of this process (50). Indeed, the investigation of experimental studies in this context has revealed that CN suppresses apoptotic cell death by decreasing the expression of Bax protein, one of the pro-apoptotic markers (47,51,52). CN treatment was found to significantly improve histopathological damage, significantly suppress oxidative stress by reducing ROS and MDA content, and increase the activity of antioxidant enzymes such as SOD and CAT in kidney tissue in a study that investigated the effects of CN on cisplatin-induced kidney damage in rats (19). In a study evaluating the protective effect of eucalyptol against gentamicin-induced renal damage, it was reported that eucalyptol administration led to a significant increase in glutathione peroxidase (GPx) and CAT activities and markedly diminished gentamicin-induced histopathological alterations. In the same study, eucalyptol was shown to suppress the inflammatory response by reducing NF-κB, TNF-α, and IL-1β expression, thereby contributing to kidney damage reduction (22). A different study demonstrated that CN and vitamin E treatment after gentamicin-induced nephrotoxicity markedly decreased TNF-α and IL-6 gene expression, as well as alleviated histological damage in renal proximal tubules and glomeruli (53).

In our study, we observed that CN treatment significantly improved oxidative stress markers in rats exposed to PD. In the PD+CN group, MDA levels were markedly diminished in comparison to the PD group, whereas GSH levels, along with SOD and CAT activity, indicative of the antioxidant defense system in renal tissue, were dramatically elevated. Additionally, our results indicated that CN administration had regulatory effects on apoptosis and the inflammatory response. The PD+CN group showed a significant decrease in Bax expression, TNF-α levels, and NF-κB activity in comparison to the PD group. Nevertheless, histopathological examinations demonstrated that the average histopathological damage scores markedly improved, and the renal tissue damage observed in the PD group was significantly reduced with CN administration. These results indicate that CN has the potential to exert nephroprotective effects in renal tissue by suppressing apoptotic processes, inflammation, and oxidative stress in PD-induced nephrotoxicity.

A limitation of the present study is that apoptosis was evaluated only through Bax immunoreactivity. Although the assessment of Bcl-2 expression and the Bax/Bcl-2 ratio could have provided a more comprehensive evaluation of apoptotic pathways, these analyses were beyond the scope of the current study and should be addressed in future investigations.

Conclusion

This study examined the protective effects of CN treatment on renal tissue in a PD-induced nephrotoxicity model. The biochemical, histopathological, and immunohistochemical results demonstrated that PD exposure induces oxidative stress, inflammation, and apoptosis processes in renal tissue, resulting in substantial damage. Conversely, the antioxidant defense system was bolstered, inflammatory markers and Bax expression were suppressed, and the histopathological damage observed in renal tissue was significantly reduced by CN treatment. These findings indicate that CN has the potential to serve as a nephroprotective agent against PD-induced nephrotoxicity by modulating apoptotic processes, inflammation, and oxidative stress. Nevertheless, additional experimental and clinical research is required to elucidate the mechanisms that underlie the renal protective effects of CN in greater detail.

Author Contributions

Concept, design, data collection, analysis and interpretation: **Tansu Kuşat, Feyza Başak, Eyüp Altınöz, Yasemin Biçer** Literature search: **Tansu Kuşat, Feyza Başak, Eyüp Altınöz,** Writing: **Tansu Kuşat,** Approval: **Eyüp Altınöz**. The authors confirm that the data supporting the findings of this study are available in the article.

Conflicts of Interest

No conflict of interest is reported by authors.

Funding

This work was supported by the Karabuk University Scientific Research Fund [KBÜBAP-25-DS-172].

Ethical Approval

Ethical approval for the study was obtained from the Karabük University Local Ethics Committee for Animal Experiments (Protocol No: 2025/10/33).

REFERENCES

1. Salama AAA, Mostafa RE, Elgohary R. Effect of L-carnitine on potassium dichromate-induced nephrotoxicity in rats: modulation of PI3K/AKT signaling pathway. Res Pharm Sci. 2022;17(2):153-163. https://doi.org/10.4103/1735-5362.335174

2. Orhan S, Turkmen R, Demirel HH, Akosman MS, Turkmen T, Fırat F. Chlorogenic acid mitigates potassium dichromate-induced acute hepato-nephrotoxicity by attenuating the NF-κB signalling pathway. Mol Biol Rep. 2024;51(1):798. https://doi.org/10.1007/s11033-024-09717-w
3. Mishra S, Bharagava RN. Toxic and genotoxic effects of hexavalent chromium in environment and its bioremediation strategies. J Environ Sci Health C Environ Carcinog Ecotoxicol Rev. 2016;34(1):1-32. https://doi.org/10.1080/10590501.2015.1096883
4. Cuevas-Magaña MY, Vega-García CC, León-Contreras JC, Hernández-Pando R, Zazueta C, García-Niño WR. Ellagic acid ameliorates hexavalent chromium-induced renal toxicity by attenuating oxidative stress, suppressing TNF-α and protecting mitochondria. Toxicol Appl Pharmacol. 2022;454:116242. https://doi.org/10.1016/j.taap.2022.116242
5. Momo CMM, Ferdinand N, Bebe NKO, Marquise MNA, Augustave K, Narcisse VB, et al. Oxidative effects of potassium dichromate on biochemical, hematological characteristics, and hormonal levels in rabbit doe (Oryctolagus cuniculus). Vet Sci. 2019;6(1):30. https://doi.org/10.3390/vetsci6010030
6. Balali-Mood M, Naseri K, Tahergorabi Z, Khazdair MR, Sadeghi M. Toxic mechanisms of five heavy metals: mercury, lead, chromium, cadmium, and arsenic. Front Pharmacol. 2021;12:643972. https://doi.org/10.3389/fphar.2021.643972
7. Zhuge R, Zhang L, Xue Q, Wang R, Xu J, Wang C, et al. Ferritinophagy is involved in hexavalent chromium-induced ferroptosis in Sertoli cells. Toxicol Appl Pharmacol. 2024;492:117139. https://doi.org/10.1016/j.taap.2024.117139
8. Sharma P, Singh SP, Parakh SK, Tong YW. Health hazards of hexavalent chromium (Cr (VI)) and its microbial reduction. Bioengineered. 2022;13(3):4923-4938. https://doi.org/10.1080/21655979.2022.2037273
9. Feng H, Feng Q, Xiao T, Liu T, Guan B, Firdous SM, et al., editors. Ipomoea staphylina attenuates potassium Dichromate-Induced nephrotoxicity in Wistar rats via antioxidant and antiapoptotic effects. Dokl Biochem Biophys. 2021;499(1):289-295. https://doi.org/10.1134/S1607672921040074
10. Awoyomi OV, Adeoye YD, Oyagbemi AA, Ajibade TO, Asenuga ER, Gbadamosi IT, et al. Luteolin mitigates potassium dichromate-induced nephrotoxicity, cardiotoxicity and genotoxicity through modulation of Kim-1/Nrf2 signaling pathways. Environ Toxicol. 2021;36(11):2146-2160. https://doi.org/10.1002/tox.23329
11. Mehany HA, Abo-Youssef AM, Ahmed LA, Arafa E-SA, Abd El-Latif HA. Protective effect of vitamin E and atorvastatin against potassium dichromate-induced nephrotoxicity in rats. Beni-Suef University J Basic Appl Sci. 2013;2(2):96-102. https://doi.org/10.1016/j.bjbas.2013.02.002
12. El-Shoura EAM, Salem MA, Ahmed YH, Ahmed LK, Zaafar D. Combined β-sitosterol and trimetazidine mitigate potassium dichromate-induced cardiotoxicity in rats through the interplay between NF-κB/AMPK/mTOR/TLR4 and HO-1/NADPH signaling pathways. Environ Sci Pollut Res Int. 2023;30(25):67771-67787. https://doi.org/10.1007/s11356-023-27021-1
13. Valko M, Morris H, Cronin MTD. Metals, toxicity and oxidative stress. Curr Med Chem. 2005;12(10):1161-1208. https://doi.org/10.2174/0929867053764635
14. Altanam SY, Darwish N, Bakillah A. Exploring the interplay of antioxidants, inflammation, and oxidative stress: mechanisms, therapeutic potential, and clinical implications. Diseases. 2025;13(9):309. https://doi.org/10.3390/diseases13090309
15. Karhib MM, El-Sayed RA, Ghanem NF, El-Demerdash FM. Nephroprotective role of echinacea purpurea against potassium dichromate-induced oxidative stress, inflammation, and apoptosis in rats. Environ Toxicol. 2022;37(9):2324-2334. https://doi.org/10.1002/tox.23599
16. Mehmeti I, Lenzen S, Lortz S. Modulation of Bcl-2-related protein expression in pancreatic beta cells by pro-inflammatory cytokines and its dependence on the antioxidative defense status. Mol Cell Endocrinol. 2011;332(1-2):88-96. https://doi.org/10.1016/j.mce.2010.09.017
17. Moomin A, Mensah KB, Forkuo AD, Adu-Gyamfi PKT, Ansah C. Ethanolic stem bark extract of terminalia ivorensis A. Chev. protects against potassium dichromate-induced nephrotoxicity in rats. Scientific African. 2020;8:e00410. https://doi.org/10.1016/j.sciaf.2020.e00410
18. Cai ZM, Peng JQ, Chen Y, Tao L, Zhang YY, Fu LY, et al. 1, 8-Cineole: a review of source, biological activities, and application. J Asian Nat Prod Res. 2021;23(10):938-954. https://doi.org/10.1080/10286020.2020.1839432
19. Kazak F, Deveci MZY, Akçakavak G. Eucalyptol alleviates cisplatin-induced kidney damage in rats. Drug Chem Toxicol. 2024;47(2):172-179. https://doi.org/10.1080/01480545.2022.2156530
20. Izham MNM, Hussin Y, Rahim NFC, Aziz MNM, Yeap SK, Rahman HS, et al. Physicochemical characterization, cytotoxic effect and toxicity evaluation of nanostructured lipid carrier loaded with eucalyptol. BMC Complement Med Ther. 2021;21(1):254. https://doi.org/10.1186/s12906-021-03422-y
21. Caldas GFR, Limeira MMF, Araújo AV, Albuquerque GS, da Costa Silva-Neto J, da Silva TG, et al. Repeated-doses and reproductive toxicity studies of the monoterpene 1, 8-cineole (eucalyptol) in Wistar rats. Food Chem Toxicol. 2016;97:297-306. https://doi.org/10.1016/j.fct.2016.09.020
22. Akcakavak G, Kazak F, Karatas O, Alakus H, Alakus I, Kirgiz O, et al. Eucalyptol regulates Nrf2 and NF-kB signaling and alleviates gentamicin-induced kidney injury in rats by downregulating oxidative stress, oxidative DNA damage, inflammation, and apoptosis. Toxicol Mech Methods. 2024;34(4):413-422. https://doi.org/10.1080/15376516.2023.2297234
23. Uyar A, Cellat M, Kanat Ö, Etyemez M, Kutlu T, Deveci MZY, et al. Bisphenol AF caused reproductive toxicity in rats and cineole co-treatment exhibited protective effect. Reprod Sci. 2024;31(11):3462-3474. https://doi.org/10.1007/s43032-024-01677-7
24. Nagy AM, Abdelhameed MF, Rihan S, Diab KA, El-Saied M, Mohamed SS, et al. Rosemary officinalis extract mitigates potassium dichromate-induced testicular degeneration in male rats: Insights from the Nrf2 and its target genes signaling pathway. Toxicol Rep. 2024;13:101700. https://doi.org/10.1016/j.toxrep.2025.101965
25. Altinoz E, Oner Z, Elbe H, Uremis N, Uremis M. Linalool exhibits therapeutic and protective effects in a rat model of doxorubicin-induced kidney injury by modulating oxidative stress. Drug Chem Toxicol. 2022;45(5):2024-2030. https://doi.org/10.1080/01480545.2021.1894751

26. Ali Hammood Keelo RM, Elbe H, Bicer Y, Yigitturk G, Koca O, Karayakali M, et al. Treatment with crocin suppresses diabetic nephropathy progression via modulating TGF-β1 and oxidative stress in an experimental model of pinealectomized diabetic rats. Chem Biol Interact. 2022;351:109733. https://doi.org/10.1016/j.cbi.2021.109733
27. Ozturk I, Elbe H, Bicer Y, Karayakali M, Onal MO, Altinoz E. Therapeutic role of melatonin on acrylamide-induced hepatotoxicity in pinealectomized rats: Effects on oxidative stress, NF-κB signaling pathway, and hepatocellular proliferation. Food Chem Toxicol. 2023;174:113658. https://doi.org/10.1016/j.fct.2023.113658
28. Prasad S, Yadav KK, Kumar S, Gupta N, Cabral-Pinto MMS, Rezania S, et al. Chromium contamination and effect on environmental health and its remediation: A sustainable approaches. J Environ Manage. 2021;285:112174. https://doi.org/10.1016/j.jenvman.2021.112174
29. Reif BM, Murray BP. Chromium toxicity. StatPearls [Internet]: StatPearls Publishing; 2024. PMID: 38261677.
30. Zhang T, Feng L, Cui J, Tong W, Zhao H, Wu T, et al. Hexavalent chromium induces neurotoxicity by triggering mitochondrial dysfunction and ROS-mediated signals. Neurochem Res. 2024;49(3):660-669. https://doi.org/10.1007/s11064-023-04063-y
31. Das J, Sarkar A, Sil PC. Hexavalent chromium induces apoptosis in human liver (HepG2) cells via redox imbalance. Toxicol Rep. 2015;2:600-608. https://doi.org/10.1016/j.toxrep.2015.03.013
32. Mohamed AAR, El-Houseiny W, Abd Elhakeem EM, Ebraheim LL, Ahmed AI, Abd El-Hakim YM. Effect of hexavalent chromium exposure on the liver and kidney tissues related to the expression of CYP450 and GST genes of Oreochromis niloticus fish: Role of curcumin supplemented diet. Ecotoxicol Environ Saf. 2020;188:109890. https://doi.org/10.1016/j.ecoenv.2019.109890
33. Zhang S, Zhao X, Hao J, Zhu Y, Wang Y, Wang L, et al. The role of ATF6 in Cr (VI)-induced apoptosis in DF-1 cells. J Hazard Mater. 2021;410:124607. https://doi.org/10.1016/j.jhazmat.2020.124607
34. El-Demerdash FM, El-Sayed RA, Abdel-Daim MM. Rosmarinus officinalis essential oil modulates renal toxicity and oxidative stress induced by potassium dichromate in rats. J Trace Element Med Biol. 2021;67:126791. https://doi.org/10.1016/j.jtemb.2021.126791
35. Balakrishnan R, Kumar CSS, Rani MU, Srikanth MK, Boobalan G, Reddy AG. An evaluation of the protective role of α-tocopherol on free radical induced hepatotoxicity and nephrotoxicity due to chromium in rats. Indian J Pharmacol. 2013;45(5):490-495. https://doi.org/10.4103/0253-7613.117778
36. Li N, Li X, Zhang X, Zhang L, Wu H, Yu Y, et al. Low-dose hexavalent chromium induces mitophagy in rat liver via the AMPK-related PINK1/Parkin signaling pathway. PeerJ. 2024;12:e17837. https://doi.org/10.7717/peerj.17837
37. Avila-Rojas SH, Aparicio-Trejo OE, Briones-Herrera A, Medina-Campos ON, Reyes-Fermín LM, Martínez-Klimova E, et al. Alterations in mitochondrial homeostasis in a potassium dichromate model of acute kidney injury and their mitigation by curcumin. Food Chem Toxicol. 2020;145:111774. https://doi.org/10.1016/j.fct.2020.111774
38. Hegazy R, Salama A, Mansour D, Hassan A. Renoprotective effect of lactoferrin against chromium-induced acute kidney injury in rats: involvement of IL-18 and IGF-1 inhibition. PLoS One. 2016;11(3):e0151486. https://doi.org/10.1371/journal.pone.0151486
39. Goodarzi Z, Karami E, Ahmadizadeh M. Simvastatin attenuates chromium-induced nephrotoxicity in rats. J Nephropathol. 2017;6(1):5-9. https://doi.org/10.15171/jnp.2017.02
40. Wang Y, Wu W, Yao C, Lou J, Chen R, Jin L, et al. Elevated tissue Cr levels, increased plasma oxidative markers, and global hypomethylation of blood DNA in male S prague-D awley rats exposed to potassium dichromate in drinking water. Environ Toxicol. 2016;31(9):1080-1090. https://doi.org/10.1002/tox.22117
41. Alanazi ST, Salama SA, Althobaiti MM, Almalki AM, Bakhsh A, Musa A, et al. Ferulic acid ameliorates chromium-induced nephrotoxicity: Modulation of PERK/eIF2α/ATF4/CHOP, Nrf2, and inflammatory signaling. Biol Trace Elem Res. 2025;203(11):5974-5986. https://doi.org/10.1007/s12011-025-04618-w
42. Liu T, Zhang L, Joo D, Sun S-C. NF-κB signaling in inflammation. Signal Transduct Target Ther. 2017;2(1):1-9. https://doi.org/10.1038/sigtrans.2017.23
43. Sahu BD, Koneru M, Bijargi SR, Kota A, Sistla R. Chromium-induced nephrotoxicity and ameliorative effect of carvedilol in rats: Involvement of oxidative stress, apoptosis and inflammation. Chem Biol Interact. 2014;223:69-79. https://doi.org/10.1016/j.cbi.2014.09.009
44. Saygılı SK, Akcilar R. Phoenixin-14 modulates Nrf2/HO-1, NF-κB, and apoptotic pathways in a rat model of monosodium glutamate-induced neurotoxicity. J Biochem Mol Toxicol. 2026;40(3):e70755. https://doi.org/10.1002/jbt.70755
45. Hoch CC, Petry J, Griesbaum L, Weiser T, Werner K, Ploch M, et al. 1, 8-cineole (eucalyptol): A versatile phytochemical with therapeutic applications across multiple diseases. Biomed Pharmacother. 2023;167:115467. https://doi.org/10.1016/j.biopha.2023.115467
46. De Vincenzi M, Silano M, De Vincenzi A, Maialetti F, Scazzocchio B. Constituents of aromatic plants: eucalyptol. Fitoterapia. 2002;73(3):269-275. https://doi.org/10.1016/S0367-326X(02)00062-X
47. Moghadam Aghajari H, Asle-Rousta M. Eucalyptol alleviates lead-induced nephrotoxicity in rats by suppressing oxidative stress, inflammation, and apoptosis, and enhancing the Nrf2/HO-1 signaling pathway. Biol Trace Elem Res. 2025. https://doi.org/10.1007/s12011-025-04831-7
48. Xu G, Guo J, Sun C. Eucalyptol ameliorates early brain injury after subarachnoid haemorrhage via antioxidant and anti-inflammatory effects in a rat model. Pharm Biol. 2021;59(1):112-118. https://doi.org/10.1080/13880209.2021.1876101
49. Jiang Z, Guo X, Zhang K, Sekaran G, Cao B, Zhao Q, et al. The essential oils and eucalyptol from Artemisia vulgaris L. prevent acetaminophen-induced liver injury by activating Nrf2-Keap1 and enhancing APAP clearance through non-toxic metabolic pathway. Front Pharmacol. 2019;10:782. https://doi.org/10.3389/fphar.2019.00782
50. Mustafa M, Ahmad R, Tantry IQ, Ahmad W, Siddiqui S, Alam M, et al. Apoptosis: A comprehensive overview of signaling pathways, morphological changes, and physiological significance and therapeutic implications. Cells. 2024;13(22):1838. https://doi.org/10.3390/cells13221838

51. Kim DY, Kang MK, Lee EJ, Kim YH, Oh H, Kim SI, et al. Eucalyptol inhibits amyloid-β-induced barrier dysfunction in glucose-exposed retinal pigment epithelial cells and diabetic eyes. Antioxidants. 2020;9(10):1000. https://doi.org/10.3390/antiox9101000

52. Liu L, Liu X, Zhao L, Liu Y. 1, 8-cineole alleviates bisphenol A-induced apoptosis and necroptosis in bursa of Fabricius in chicken through regulating oxidative stress and PI3K/AKT pathway. Ecotoxicol Environ Saf. 2021;226:112877. https://doi.org/10.1016/j.ecoenv.2021.112877

53. Rahimi Monfared S, Valibeik A, Jafaripour L, Eslamifar Z, Veiskarami S, Ahmadvand H. Role of cineole in alleviation of acute kidney injury and renal function recovery following gentamicin administration in rats. Iran J Basic Med Sci. 2023;26(5):504-510. https://doi.org/10.22038/IJBMS.2023.68430.14944